

# 松潘-甘孜地块南缘燕山早期矽卡岩型钨钼矿床

——来自大牛场成岩成矿年代学及锆石 Hf 同位素证据\*

谭洪旗<sup>1,2,3</sup>, 朱志敏<sup>1,2,3</sup>, 周家云<sup>1,2,3</sup>, 周雄<sup>1,2,3</sup>, 胡军亮<sup>1,2,3,4</sup>, 刘应冬<sup>1,2,3</sup>

(1 中国地质科学院矿产综合利用研究所, 四川 成都 610041; 2 中国地质调查局稀土资源应用技术创新中心, 四川 成都 610041; 3 中国地质调查局金属矿产资源综合利用技术研究中心, 四川 成都 610041; 4 成都理工大学地球科学学院, 四川 成都 610059)

**摘要** 矽卡岩型矿床是钨、钼、锡等矿产的重要来源之一, 中国的矽卡岩型矿床绝大多数分布于中国东部, 成矿时代主要为燕山期。川西九龙大牛场是在松潘-甘孜地块新发现的矽卡岩型钨钼矿床, 其成岩成矿时代尚未得到精确限定。大牛场地区铁厂河花岗岩体以二长花岗岩为主, 少量正长花岗岩, 而钨钼矿体主要产于矽卡岩中。文章对该矿床开展锆石 U-Pb 定年、Hf 同位素和辉钼矿 Re-Os 定年, 结果显示铁厂河花岗岩中锆石 LA-ICP-MS U-Pb 年龄为(166.0±0.9)Ma (MSWD=0.27), 与矿石中辉钼矿 Re-Os 加权平均年龄((166.8±1.7)Ma, MSWD=0.90)在误差范围内基本一致, 成岩成矿时代是燕山早期; 锆石  $\epsilon_{\text{Hf}}(t)$  为-10.69~4.37 (平均 0.82), 模式年龄  $T_{\text{DM2}}$  为 1229~931 Ma (平均 1099 Ma) 和 1884 Ma, 表明该花岗岩为扬子地块基底元古代与中元古代地壳重熔形成的。结合前人在该区获得的成岩成矿年龄, 反映研究区内 166 Ma 左右存在一期与花岗岩浆有关的钨钼成岩成矿事件, 这一发现为川西九龙地区及其周缘矿产勘探拓宽了思路。

**关键词** 地球化学; 辉钼矿 Re-Os; 锆石 U-Pb; 花岗岩; 松潘-甘孜; 川西  
**中图分类号**: P618.65; P618.67 **文献标志码**: A

## Early Yanshanian skarn W-Mo deposit in the southern margin of Songpan-Ganze terrane: Evidence from diagenetic and metallogenic chronology, zircon Hf isotopes in Daniuchang area

TAN HongQi<sup>1,2,3</sup>, ZHU ZhiMin<sup>1,2,3</sup>, ZHOU JiaYun<sup>1,2,3</sup>, ZHOU Xiong<sup>1,2,3</sup>, HU JunLiang<sup>1,2,3,4</sup> and LIU YingDong<sup>1,2,3</sup>

(1 Institute of Multipurpose Utilization of Mineral Resources, CAGS, Chengdu 610041, Sichuan, China; 2 Technical Innovation Center of Rare Earth Resources, China Geological Survey, Chengdu 610041, Sichuan, China; 3 Research Center of Multipurpose Utilization of Metal Mineral Resources of China Geological Survey, Chengdu 610041, Sichuan, China; 4 College of Earth Sciences, Chengdu University of Technology, Chengdu 610059, Sichuan, China)

### Abstract

Skarn deposits are an important source of W, Mo, Sn, and other minerals. Most of the skarn deposits in China are distributed in eastern China, and the metallogenic epoch is mainly Yanshanian. The Daniuchang W-Mo deposit, located in the Jiulong region of the western Sichuan Province, is a newly discovered skarn deposit in the Songpan-Ganze terrane, and its genesis is rarely studied. The Tiechanghe granitoids in Daniuchang area are mainly monzogranite with a small amount of syenogranite, while the tungsten and molybdenum ore bodies mainly occur in skarn. In this paper, zircon U-Pb dating, Hf isotope and molybdenite Re-Os dating are carried out

\* 本文得到国家自然科学基金项目(编号:41603034)和中国地质调查局项目(编号:DD20190185、DD20221697)共同资助  
第一作者简介 谭洪旗,男,1984年生,高级工程师,主要从事岩石地球化学研究。Email:hongqitan@163.com  
收稿日期 2021-06-21;改回日期 2021-12-23。张绮玲编辑。

for the samples from the deposit. The result shows that the zircon LA-ICP-MS U-Pb age for Tiechanghe granite is  $(166.0 \pm 0.9)$  Ma (MSWD=0.27), which is basically consistent with the molybdenite Re-Os weighted average age for ores  $((166.8 \pm 1.7)$ Ma, MSWD=0.90), The age of intrusion / mineralization is Early Yanshanian. The zircon  $\varepsilon_{\text{Hf}}(t)$  ranges from  $-10.69$  to  $4.37$  (average 0.84), and the model ages range from 1229 Ma to 931 Ma (average 1099 Ma) and 1884 Ma, suggesting that the granite may have been formed by the remelting of the Paleoproterozoic and Mesoproterozoic crust in the basement of the Yangtze Block. Combined with the intrusion and mineralization ages published previously, there should be an important magmatic and metallogenic event of around 166 Ma forming the granitic intrusions and related W-Mo deposits in the study area. The data is helpful for mineral exploration in the Jiulong region and its surrounding areas in western Sichuan Province.

**Key words:** geochemistry, Re-Os dating of molybdenite, zircon U-Pb dating, granite, Songpan-Ganze, western Sichuan Province

矽卡岩矿床是世界上钨、钼、锡等金属矿产的重要来源(赵一鸣等,2012)。在中国,该类矿床中钨、锡、钼的储量占比分别为71%、87%、17%(Chang et al., 2019),但分布很不均匀,绝大多数分布于中国东部,是环太平洋重要成矿带之一(Mao et al., 2019)。钨是重要的战略性关键矿产之一,一般与钼矿共生,主要分布在华南地块的南岭钨锡成矿带和赣北皖南钨成矿带(蒋少涌等,2020)。其中,燕山期(180~80 Ma)的 $\text{WO}_3$ 累计探明储量可达近600万吨(夏庆霖等,2018;盛继福等,2015)。矽卡岩型钨矿床的矿体主要呈似层状、透镜状及细网脉状产于花岗岩与碳酸盐岩的内、外接触带中,由含矿热液流体交代作用而形成。矽卡岩型钨矿床往往也伴生其他多金属组合,中国典型的矽卡岩型钨矿床有湖南柿竹园钨锡钼铋多金属矿床(毛景文等,1996)、湖南新田岭钨矿床(双燕等,2016)、滇东南南秧田钨矿床(谭洪旗等,2011;蔡倩茹等,2018)等。

前人报道的川西钨矿床有康定赫德石英脉型钨矿床(杨涛等,2017)、雪宝顶石英脉型W-Sn-Be矿床(刘琰等,2007;Liu et al., 2012),其余石英脉型和云英岩型钨锡矿规模均很小,不具开采价值。20世纪70年代,松潘-甘孜南缘江浪穹隆北缘发现了大牛场矽卡岩型白钨矿矿床,多年来找矿未有进展;近年来,在该区矽卡岩类矿床中又发现了辉钼矿矿体。这些发现结束了松潘-甘孜地块少有燕山早期矽卡岩型钨矿床的报道。

本文在铁厂河花岗岩体LA-ICP-MS锆石U-Pb定年和Hf同位素的基础上,结合辉钼矿Re-Os定年,精确厘定大牛场W-Mo矿床的成岩成矿时代,探讨了矿床成因,总结成矿规律,对指导江浪穹隆及其周围的找矿勘探工作具有重要意义。

## 1 区域地质背景

川西江浪地区位于扬子地块西缘与松潘-甘孜造山带的结合部位,是木里-盐源弧形构造带的组成部分(图1),以发育孤立分散状产出的江浪变质穹隆地质体为特征(颜丹平等,1997;侯立玮,1996;2002)。这些变质穹隆形成于被动大陆边缘拉张环境(颜丹平等,1997;侯立玮,1996;侯立玮等,2002;谭洪旗,2019),经历了多期复杂构造-变质热事件的改造,约10 Ma开始隆升、剥蚀至地表(谭洪旗,2019)。江浪穹隆以发育里伍式铜锌矿床著称(谭洪旗等,2013;Zhou et al, 2017),东部产有青纳-锦屏韧性剪切带型金矿床,如青纳、茶铺子、张家坪子等金矿床(谭洪旗等,2016),以及牦牛坪稀土矿床;因此,以青纳-锦屏韧性剪切带为分界,有着“西铜中金东稀”的矿床分布特点。区域上,该区主要分布奥陶纪—三叠纪地层(谭洪旗,2019),以三叠系西康群为主,包括扎尕山组、新都桥组和侏倭组。大牛场矿床分布在江浪穹隆的倾末端,矿区东南部为向北东倾斜的单层,隶属河口向斜南西翼部分,岩层倾角在 $40^\circ$ 左右;矿区的西南部为平缓向斜褶皱,南翼岩层倾角为 $30^\circ \sim 40^\circ$ ,而北翼倾角仅 $15^\circ$ 左右。该向斜轴呈北东方向大致顺出龙沟西侧延伸,向东受到河口向斜制约而渐趋消失,其次是叠加于该向斜翼上与之直正交的NNW向挠曲及倾角在 $15^\circ$ 左右的平缓背斜、向斜构造。

矿区周边存在印支期(220~205 Ma)I型和燕山早期(165~150 Ma)A型花岗岩(罗丽萍等,2021)。其中印支期(220~205 Ma)I型花岗岩有兰尼巴岩体、羊房沟岩体、三岩龙-放马坪岩体、嘎啦子岩体等(万传辉等,2011;袁静等,2011;刘大明,2018),燕山早

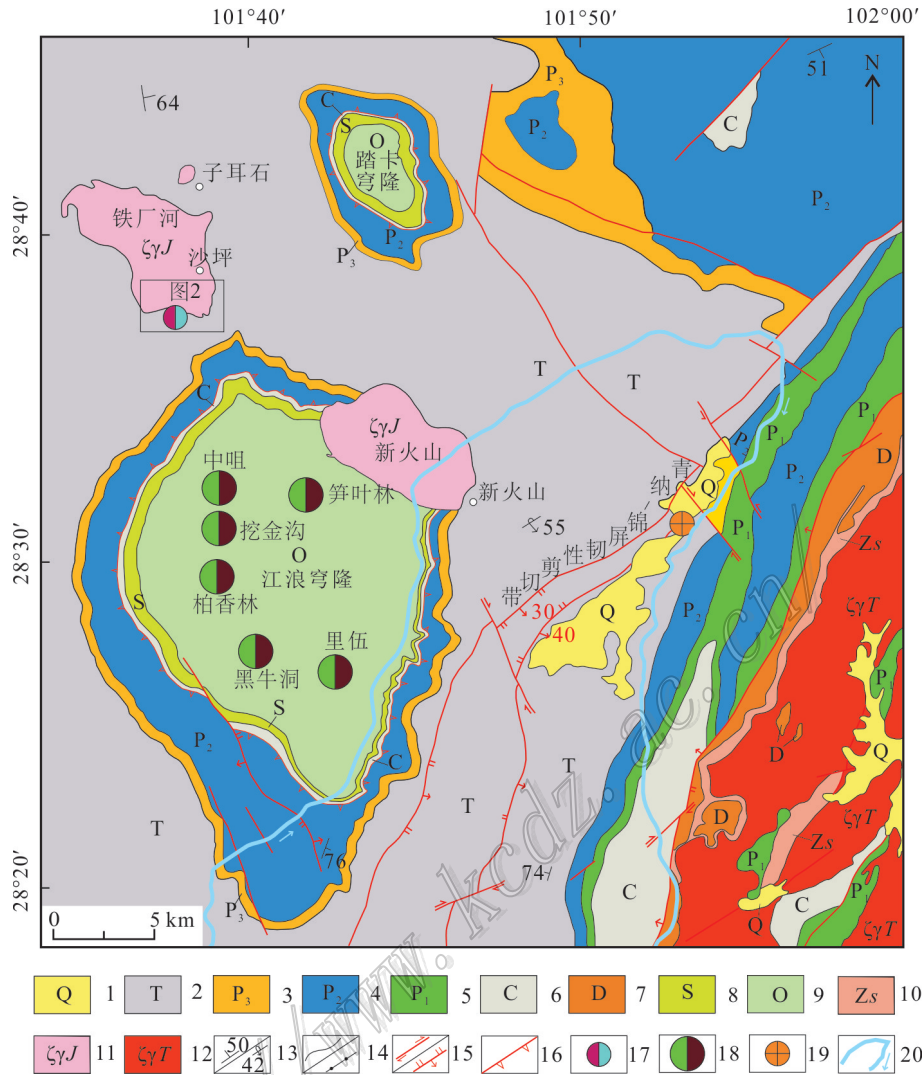


图1 川西江浪穹隆及其邻区地质略图

- 1—第四系松散堆积物;2—三叠系片岩和板岩;3—上二叠统砂板岩;4—中二叠统玄武岩;5—下二叠统灰岩;6—石炭系硅质条带、石英岩;
- 7—泥盆系硅质岩和板岩;8—志留系硅质岩、石英岩;9—奥陶系片岩、石英岩;10—苏雄组凝灰岩;11—侏罗纪花岗岩;12—新元古代花岗岩;
- 13—正常产状和倒转产状;14—实测地质界线和角度不整合地质界线;15—实测平移断层和实测逆断层;16—剥离断层;17—钨钼矿床;
- 18—铜锌矿床;19—金矿床;20—雅砻江及其水流方向

Fig.1 Geologic sketch map of the Jianglang dome and its adjacent areas in western Sichuan

- 1—Quaternary loose sediments; 2—Triassic schist and slate; 3—Upper Permian sandy slate;4—Middle Permian basalt; 5—Lower Permian limestone; 6—Carboniferous siliceous bands and quartzite; 7—Devonian siliceous rock and slate; 8—Silurian Siliceous rock and quartzite; 9—Ordovician schist and quartzite; 10—Tuff of Suxiong Formation; 11—Jurassic granite;12—Neoproterozoic granite; 13—Normal and reversed attitude; 14—Measured geologic boundary and angular unconformity boundary; 15—Measured strike slip fault and measured reverse fault; 16—Detachment faults; 17—Tungsten molybdenum deposit; 18—Copper-zinc deposit; 19—Gold deposit; 20—Yalong River and its water flow direction

期(165~150 Ma)A型花岗岩有新火山岩体(又称文家坪)、铁厂河岩体(又称乌拉溪岩体)和桥棚子岩体(周家云等,2013;2014a;谭洪旗,2019;刘晓佳等,2021)。变质作用早期以区域变质作用(低绿片岩相)为主,后发育以围绕江浪穹隆的巴罗式变质作用(谭洪旗,2019)。另外,区域上发育以里伍、黑牛洞、

挖金沟、中咀、笋叶林等矿床组成的“里伍式铜锌矿田”及与燕山早期A型花岗岩有关的锂铍和钨钼矿床(谭洪旗,2019;胡军亮等,2020),这些矿床年龄限制在166~150 Ma(Zhou et al., 2017;谭洪旗,2019)。总之,川西九龙地区的矿床主要集中在燕山期,以Cu-Zn-W-Mo-稀有金属矿化为特征。

### 2 矿床地质

大牛场矿区出露地层为三叠系西康群扎尕山组,总体为一套变质砂岩、板岩夹大理岩(图2)。矿区构造简单,仅见一些平缓的小褶曲(图3a)。矿区内有铁厂河岩体,分布于铁厂河及九龙河交汇一带,呈纺锤型岩株侵入,长轴近南北向,主要岩性有二长花岗岩和正长花岗岩。该岩体内部多发育2组节理,1组产状为 $310^{\circ}\sim 330^{\circ}\angle 50^{\circ}\sim 60^{\circ}$ ,另一组产状为 $55^{\circ}\sim 70^{\circ}\angle 65^{\circ}\sim 75^{\circ}$ ,节理面平直,未见矿物充

填;且岩体内部分布有伟晶岩脉,宽5~80 cm,长数米至100 m规模不等。岩体与围岩表现为侵入接触,接触界面向外陡倾,围岩周边发育50~100 m不等的热接触变质带,蚀变岩石有阳起透辉钠长石岩、黑云石英角岩、角岩化砂岩、云母片岩、矽卡岩等(图2)。

矿区早期经历了区域变质作用,后期由于花岗岩体的侵入,发生热接触变质。岩石类型有角岩、矽卡岩、片岩、大理岩等。其中矽卡岩类型有阳起石-石榴子石矽卡岩、石榴子石透辉石(含钙铁辉石)矽卡岩、透辉石-钙铁辉石矽卡岩、稀疏磁黄铁矿化透

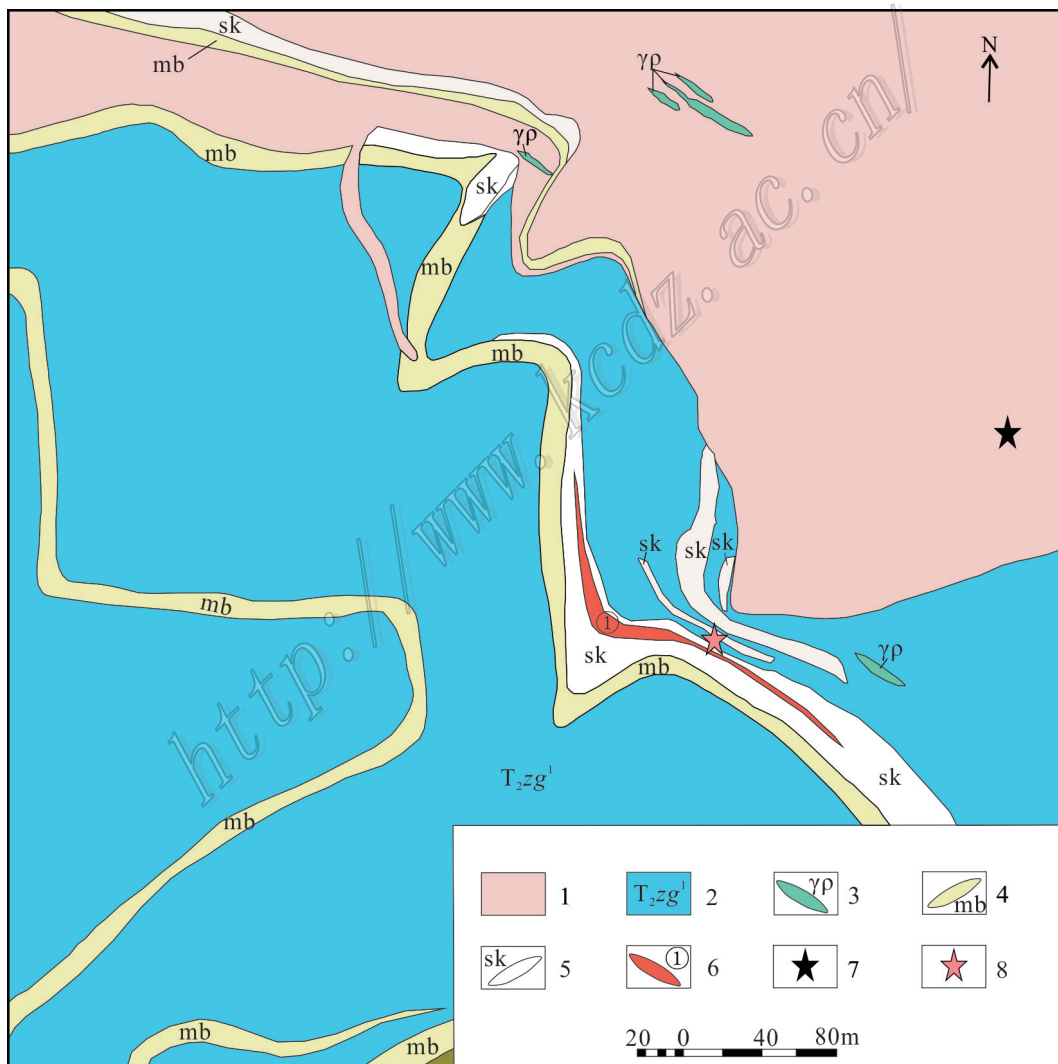


图2 大牛场矿区地质图及采样位置

1—铁厂河花岗岩;2—扎尕山组一段板岩;3—花岗伟晶岩;4—大理岩;5—矽卡岩;6—钨钼矿体;7—花岗岩采样位置;8—辉钼矿采样位置

Fig.2 Geologic map and sample location of the Daniuchang mining area

1—Tiechanghe granite; 2—The first member of Zhagashan Formation, slate; 3—The granite pegmatite; 4—Marble; 5—Skarn; 6—Tungsten-molybdenum ore body; 7—Sample location of granite; 8—Sample location of molybdenite

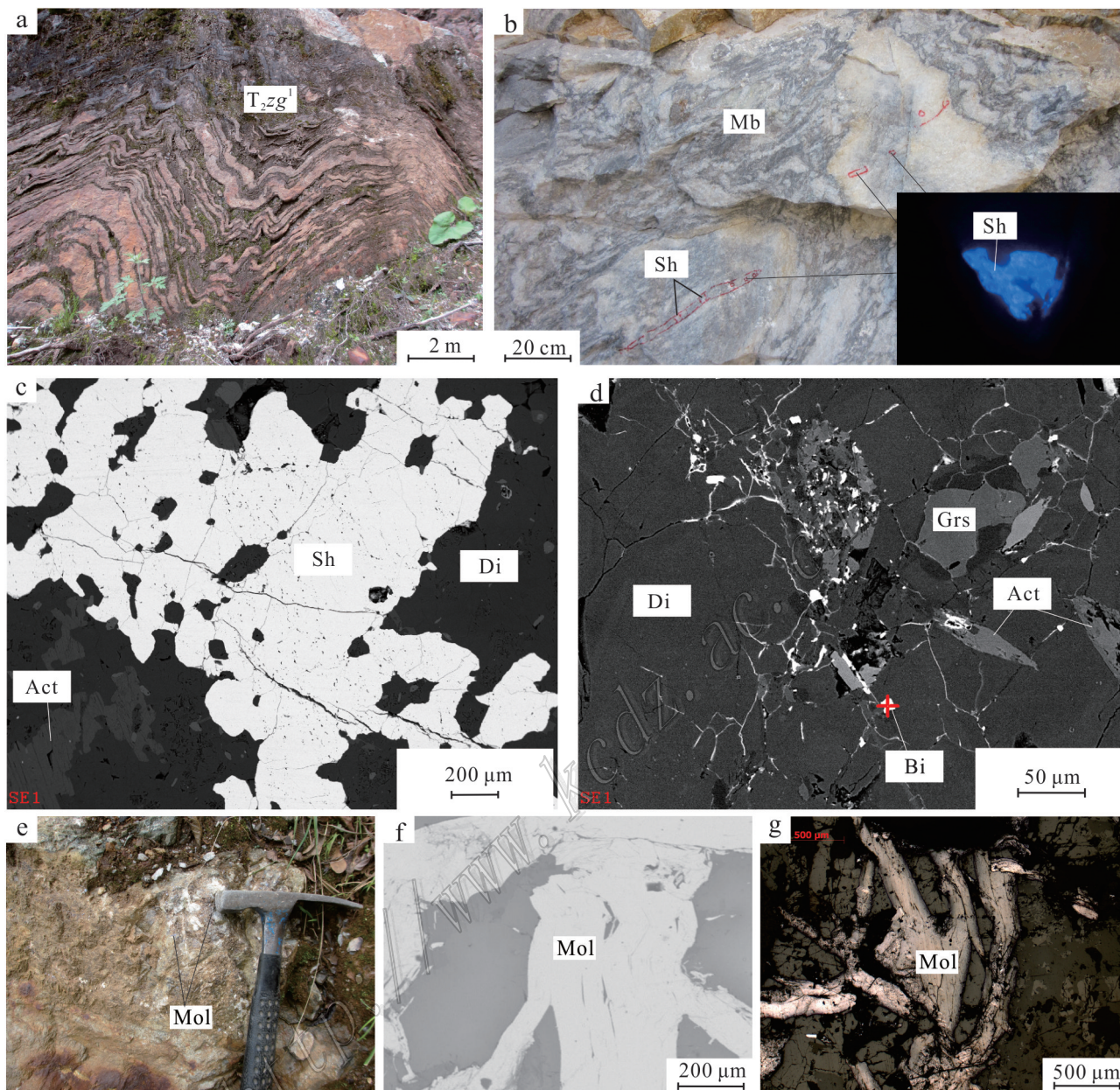


图3 大牛场矿区构造变形、矿石矿物组成

a. 三叠系扎尕山组一段( $T_{2zg^1}$ )岩层变形;b. 条带状白钨矿,紫外灯下显天蓝色荧光;c,d. 扫描电镜下矿石矿物组成,c为含白钨矿矽卡岩,d为含自然铋的矽卡岩;e. 含辉钼矿矽卡岩;f,g. 放射状辉钼矿,有变形特征

Act—阳起石;Sh—白钨矿;Di—辉石;Bi—铋;Grs—钙铝榴石;Mol—辉钼矿;Mb—大理岩

Fig.3 Structural deformation and ore minerals in the Daniuchang mining area

a. Strata deformation in First Member of Triassic Zhagashan ( $T_{2zg^1}$ ) Formation; b. Banded scheelite, sky blue fluorescence under UV lamp; c, d. Ore mineral composition under scanning electron microscope, c is scheelite skarn, and d is natural bismuth-bearing skarn; e. Molybdenite skarn; f, g. Radial molybdenite with deformation characteristics

Act—Actinolite; Sh—Scheelite; Di—Diopside; Bi—Bismuth; Grs—Grossularite; Mol—Molybdenite; Mb—Marble

辉石矽卡岩、褐铁矿化石榴子石-透辉石矽卡岩、石榴子石矽卡岩、透闪石矽卡岩、符山石矽卡岩等。岩石一般为灰绿色、具粒状变晶结构,块状、条带状

构造。主要脉石矿物有钙铝榴石、铁铝榴石、透辉石、钙铁辉石、符山石,次要矿物为绿帘石、黝帘石、阳起石、云母、方解石、电气石、萤石、金属矿物赤铁

矿、闪锌矿、磁黄铁矿等。

矿区发现4条矿体(周家云等,2014b),主要赋存在矽卡岩和石英脉中,呈层状、似层状及透镜状产出(图2)。I-III号矿体位于矿区中部,为区内最大的一条矽卡岩带上,出露长度约1000 m,宽度大于10 m;矿体总体产状为 $120^{\circ}\angle 8^{\circ}$ ,呈似层状、透镜状赋存于层状矽卡岩内,产状与矽卡岩一致,白钨矿等矿石矿物呈浸染状分布于矽卡岩中;岩性主要为透辉石矽卡岩、透辉石-黝帘石矽卡岩,围岩为片岩、千枚岩、大理岩;白钨矿矿体品位为0.07%~0.52%(平均0.22%),厚度总计为6.37 m。IV号矿体上部为石英脉型辉钼矿体,下部为矽卡岩型辉钼矿体,地表出露宽度为2~3 m,呈层状、似层状、透镜状产出;矿体总体呈东西向展布,产状为 $131^{\circ}\angle 10^{\circ}$ ,矿体厚度2.45~7.28 m,辉钼矿矿体品位为0.14%~0.27%(平均为0.17%)。

矿床围岩蚀变有矽卡岩化、硅化,主要矿物组合有透辉石+阳起石+角闪石、斜黝帘石+透闪石+次闪石+方解石、黑云母+绿泥石+绿帘石+符山石等。矿石类型主要为层状-似层状白钨矿和辉钼矿矿石,赋矿岩石为矽卡岩化大理岩、石英脉,岩石呈灰白色略带绿色,粒状变晶结构,块状、条带状构造。矿石矿物主要为白钨矿和辉钼矿,脉石矿物为方解石、黑云母、绿泥石、绿帘石等。矿石具不等粒花岗变晶结构、花岗变晶穿插结构以及穿插-筛状变晶结构等,块状、条带状构造。其中,条带状构造主要表现为透辉石、阳起石、普通角闪石等与长石、方解石等矿物集中呈条带,或不同的暗色矿物的分别集中所致。同时,透辉石、普通角闪石、符山石、石榴子石等矿物多为穿插连生和镶嵌关系,斜黝帘石、透闪石、次闪石、方解石等常穿插交代上述矿物。扫描电镜显示,W以白钨矿的赋存状态出现(图3c),自然铋主要呈细脉状分布在透辉石矿物之间的裂隙中(图3d)。自然铋的发现,暗示该期成矿处于贫硫体系。

### 3 样品采集和分析方法

#### 3.1 样品采集及描述

7件辉钼矿样品采样位置和样品特征见图2和图3。该矿床主要矿石矿物为白钨矿和辉钼矿,伴生有少量或微量锡石、黄铜矿、方铅矿、闪锌矿、黄铁矿、磁黄铁矿等。脉石矿物主要为透辉石,其次是透

闪石、普通角闪石、钠长石、符山石、石榴子石等。白钨矿为灰白色-白色,紫外灯下显天蓝色荧光(图3b),一般呈细粒状,亦有团块状白钨矿颗粒。辉钼矿呈浸染状分布在矽卡岩表面,呈片状、束状、板片状,嵌布于石英颗粒间,辉钼矿颗粒在局部密集分布,呈斑染形式;部分为放射状辉钼矿(图3e、图3f),呈板片状产出,短径长0.05~0.15 mm,呈集合体的形式以斑点状嵌布于脉石中。

铁厂河花岗岩岩性以二长花岗岩为主,边部有少量的正长花岗岩(图4a、4b)。岩石的矿物成分主要有微斜长石(30%~40%)、更长石(25%~30%)、石英(30%±)、黑云母(3%~5%)和白云母(4%),副矿物有锆石、磷灰石、榍石等(图4a、4b)。用于LA-ICP-MS锆石U-Pb定年及Hf同位素分析的样品(样品PM07-2)采自乌拉溪乡坡上村,为灰白色中细粒二长花岗岩,矿物粒度为1~3 mm。其中,微斜长石呈半自形-他形晶,常交代更长石;更长石呈半自形晶,少数具环带构造,微斜长石交代时常发育有蠕英石(图4a);石英呈他形粒状,局部有交代更长石现象。微斜长石中发育蠕虫结构或称为蠕英石,粗的蠕虫状石英靠近钾长石,细的蠕虫状石英集中在斜长石中部,反映了粗的形成早,细的形成晚(图4a)。蠕英石成因有固溶体分离或钾长石交代斜长石等认识,Rong等(2016)认为是后来再生的斜长石交代钾长石,多余的SiO<sub>2</sub>形成含蠕状石英的蠕英石。

#### 3.2 分析方法

##### (1) 锆石U-Pb年代学及Hf同位素

样品在廊坊诚信地质服务公司经破碎、分选,双目镜下挑纯获得锆石。锆石的阴极发光显微结构照相、锆石U-Pb定年和Hf同位素由中国地质科学院矿产资源研究所成矿作用与资源评价重点实验室完成。锆石U-Pb年龄测定和Hf同位素分析在Finnigan Neptune型MC-ICP-MS上完成,激光剥蚀系统为Newwave UP 213,仪器测试条件、参数及详细分析流程见侯可军等(2009)。锆石测点同位素比值和元素含量计算采用ICPMSData(Liu et al.,2008)软件处理。年龄计算及谐和图的绘制采用Isoplot 4.15(Ludwig,2003)完成。

##### (2) 辉钼矿Re-Os同位素定年及电子探针分析

样品经粉碎、分离、粗选和精选,获得了纯度>99%的辉钼矿。辉钼矿Re-Os同位素分析在国家地质测试中心Re-Os同位素实验室由李超副研究员完成测试。辉钼矿样品采用美国TJA公司的电感耦

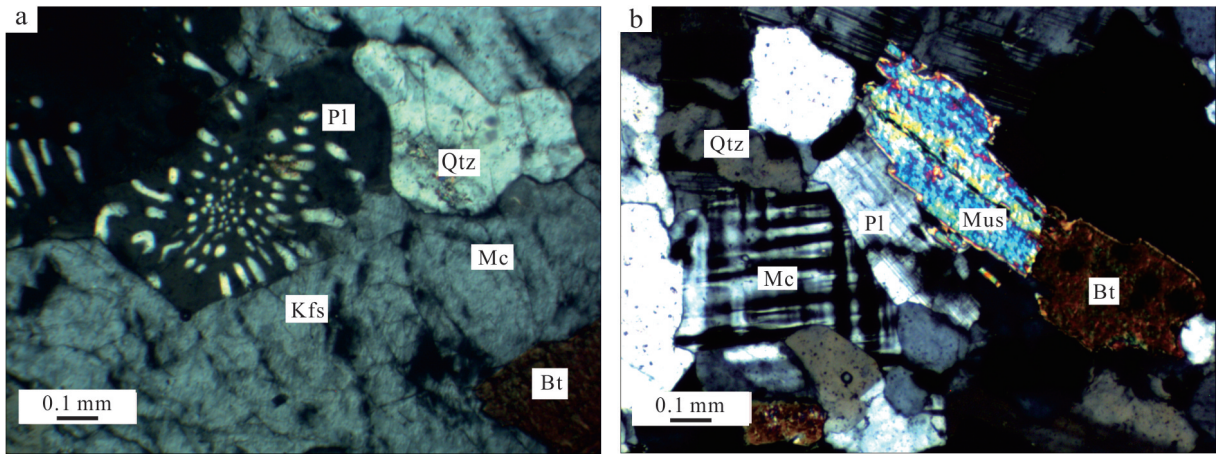


图4 乌拉溪地区铁厂河二长花岗岩(a)和正长花岗岩(b)的镜下特征(正交偏光)

Mc—微斜长石;Kfs—钾长石;Mus—白云母;Bt—黑云母;Pl—斜长石;Qtz—石英

Fig.4 Microscopic characteristics of Tiechanghe monzogranite (a) and syenogranite (b) in Wulaxi area (crossed polars)

Mc—Microcline; Kfs—Potash feldspar; Mus—Muscovite; Bt—Biotite; Pl—Plagioclase; Qtz—Quartz

合等离子体质谱仪JA X-series ICP-MS测定同位素比值。Re-Os同位素分析原理及详细分析流程参见文献(Shirey et al., 1995; 杜安道等, 2012)。电子探针分析由中国地质科学院矿产综合利用研究所王越工程师完成, 日本岛津公司生产的EMPA-1720型电子探针, 仪器工作的加速电压为25 kV, 电流为20 nA, 电子束束斑直径小于1  $\mu\text{m}$ , 分析精度0.1%。

## 4 结果

### 4.1 锆石LA-ICP-MS U-Pb同位素年龄和Hf同位素

#### 4.1.1 锆石U-Pb年龄

铁厂河花岗岩中锆石绝大多数呈无色透明、自形-半自形、正方双锥状、柱状及半截锥状, 晶体长为120~300  $\mu\text{m}$ , 宽为80~140  $\mu\text{m}$ , 长宽比约为2:1。CL图像上表现出韵律环带, 无继承锆石核, 属典型岩浆锆石。另有少量锆石发育核一边结构, 核部呈浑圆状, 边部具薄环带, 为捕获锆石。

样品PM07-2为二长花岗岩, 分析的20个测点中, 岩浆锆石15点, 捕获锆石5点(表1)。其中15点岩浆锆石 $w(\text{U})$ 为 $84 \times 10^{-6} \sim 741 \times 10^{-6}$ ,  $w(\text{Th})$ 为 $15 \times 10^{-6} \sim 352 \times 10^{-6}$ , Th/U比值为0.12~0.70, 表明其为岩浆成因锆石。15个岩浆锆石 $^{206}\text{Pb}/^{238}\text{U}$ 表面年龄为165~172 Ma(图5),  $^{206}\text{Pb}/^{238}\text{U}$ 加权平均年龄为 $(166.0 \pm 0.9) \text{Ma}$  (MSWD=0.27), 代表了乌拉溪燕山早期花岗岩浆结晶年龄。其中, 点19的 $^{206}\text{Pb}/^{238}\text{U}$

表面年龄为221 Ma, 暗示该花岗岩体捕获了印支期岩浆锆石。点17、10、4、11的 $^{206}\text{Pb}/^{238}\text{U}$ 表面年龄分别为532 Ma、606 Ma、911 Ma、915 Ma, 为继承或捕获地层中的锆石。

#### 4.1.2 锆石Hf同位素

定年样品中锆石Lu-Hf同位素原位微区测定结果列于表2。样品PM07-2锆石的 $^{176}\text{Lu}/^{177}\text{Hf}$ 为0.000 484~0.003 109(平均0.001 158),  $^{176}\text{Hf}/^{177}\text{Hf}$ 为0.282 371~0.282 800(平均0.282 697),  $\epsilon_{\text{Hf}}(t)$ 为-10.69~4.37(平均0.82), 二阶段模式年龄( $T_{\text{DM}2}$ )为931~1884 Ma(图6)。其中, 继承锆石 $^{206}\text{Pb}/^{238}\text{U}$ 表面年龄为221.2 Ma、531.5 Ma、606.2 Ma、911.2 Ma、915.4 Ma, 所对应的二阶段模式年龄分别为1992 Ma、2183 Ma、1010 Ma、2319 Ma、2133 Ma。

### 4.2 辉钼矿Re-Os同位素

电子探针测试(表3)显示, 本文中辉钼矿的 $w(\text{Mo})$ 为55.407%~56.112%(平均55.698%),  $w(\text{Re})$ 为0.073%~0.111%(平均0.091%),  $w(\text{S})$ 为41.759%~42.480%(平均41.909%),  $w(\text{Os})$ 为0.014%~0.134%(平均0.060%)。与标准辉钼矿矿物化学特征比较(王濮等, 1982), 大牛场辉钼矿的 $w(\text{Mo})$ 为4.242%,  $w(\text{S})$ 为1.849%,  $w(\text{Re})$ 约0.058%, 表明大牛场辉钼矿中Re、S等元素含量高于标准辉钼矿。

大牛场钨钼矿床7件辉钼矿的Re-Os测试结果见表4和图7。结果显示, 辉钼矿中普Os含量很低,  $w(\text{Os})$ 为 $(0.0757 \pm 0.0035) \times 10^{-9} \sim (3.585 \pm 0.042) \times 10^{-9}$ ;

表1 铁厂河花岗岩体LA-ICP-MS 锆石 U-Pb 年龄数据

Table1 LA-ICP-MS zircon U-Pb isotopic data of the Tiechanghe granite

分析点	$w(B)/10^{-6}$			Th/U	同位素比值						同位素年龄/Ma					
	Pb	Th	U		$^{207}\text{Pb}/^{206}\text{Pb}$	1 $\sigma$	$^{207}\text{Pb}/^{235}\text{U}$	1 $\sigma$	$^{206}\text{Pb}/^{238}\text{U}$	1 $\sigma$	$^{207}\text{Pb}/^{206}\text{Pb}$	1 $\sigma$	$^{207}\text{Pb}/^{235}\text{U}$	1 $\sigma$	$^{206}\text{Pb}/^{238}\text{U}$	1 $\sigma$
PM07-2																
1	32	69	172	0.40	0.05054	0.00125	0.18194	0.00445	0.02613	0.00018	220	57	170	4	166	1
2	34	66	287	0.23	0.04943	0.00035	0.17763	0.00201	0.02607	0.00024	169	17	166	2	166	2
3	39	72	193	0.37	0.04945	0.00042	0.17670	0.00225	0.02592	0.00026	169	20	165	2	165	2
4	177	45	35	1.30	0.07401	0.00110	1.55286	0.03907	0.15183	0.00213	1043	30	952	16	911	12
5	116	167	741	0.22	0.04973	0.00021	0.17950	0.00207	0.02618	0.00028	189	9	168	2	167	2
6	82	103	500	0.21	0.04949	0.00025	0.17908	0.00198	0.02625	0.00026	172	11	167	2	167	2
7	7	20	118	0.17	0.04911	0.00098	0.17532	0.00442	0.02594	0.00053	154	46	164	4	165	3
8	90	125	335	0.37	0.04977	0.00041	0.17885	0.00330	0.02605	0.00041	183	23	167	3	166	3
9	39	24	196	0.12	0.05193	0.00048	0.18662	0.00324	0.02605	0.00037	283	20	174	3	166	2
10	32	10	21	0.49	0.06203	0.00092	0.84284	0.01559	0.09859	0.00120	676	32	621	9	606	7
11	228	44	90	0.49	0.07141	0.00032	1.50257	0.01421	0.15258	0.00127	969	14	931	6	915	7
12	55	15	84	0.18	0.04988	0.00155	0.18695	0.00834	0.02709	0.00058	191	69	174	7	172	4
13	144	139	222	0.63	0.04976	0.00076	0.17855	0.00386	0.02600	0.00032	183	37	167	3	165	2
14	147	83	194	0.42	0.05112	0.00089	0.18382	0.00308	0.02611	0.00028	256	41	171	3	166	2
15	57	49	250	0.20	0.04952	0.00038	0.17751	0.00163	0.02600	0.00015	172	19	166	1	166	1
16	59	78	213	0.37	0.04958	0.00124	0.17789	0.00589	0.02599	0.00041	176	57	166	5	165	3
17	282	55	26	2.16	0.05866	0.00085	0.69550	0.01285	0.08595	0.00092	554	32	536	8	532	6
18	143	77	259	0.30	0.04944	0.00037	0.17818	0.00220	0.02615	0.00026	169	19	167	2	166	2
19	223	82	299	0.28	0.05434	0.00042	0.26669	0.00829	0.03491	0.00087	387	49	240	7	221	5
20	694	352	505	0.70	0.05006	0.00036	0.17901	0.00207	0.02596	0.00029	198	12	167	2	165	2

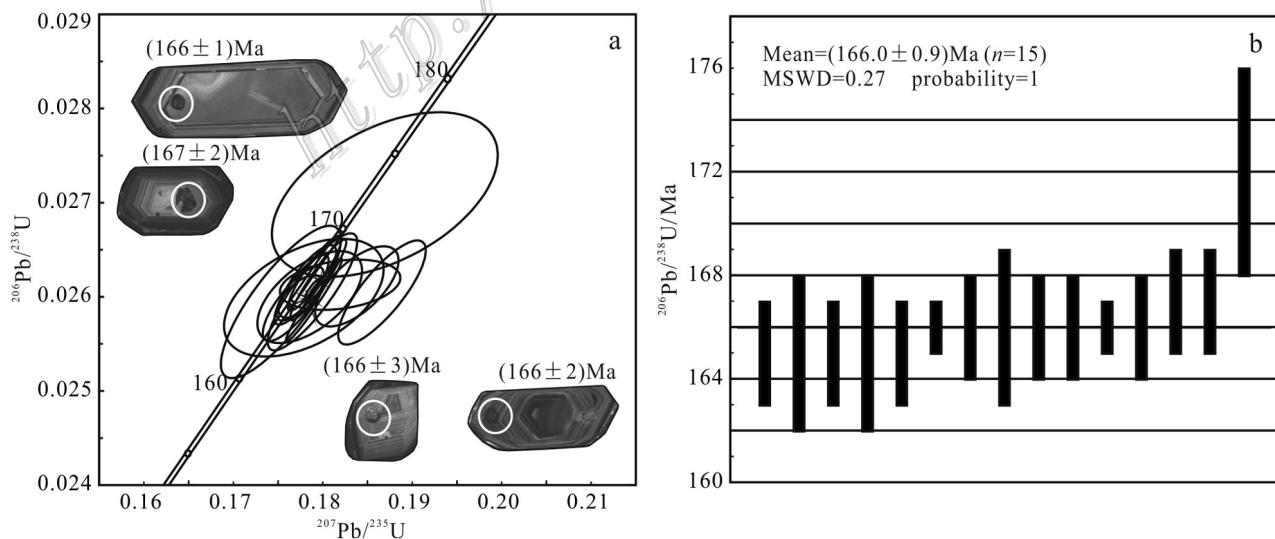


图5 铁厂河花岗岩中锆石的U-Pb年龄谐和图(a)及加权平均值图(b)

Fig.5 Zircon U-Pb concordia diagram(a)and weighted average dating (b) of the Tiechanghe granite



表 2 铁厂河花岗岩体锆石 Hf 同位素组成

Table 2 Zircon Hf isotopic compositions of the Teichanghe granite

测点	年龄/Ma	<sup>176</sup> Yb/ <sup>177</sup> Hf	2σ	<sup>176</sup> Lu/ <sup>177</sup> Hf	2σ	<sup>176</sup> Hf/ <sup>177</sup> Hf	2σ	ε <sub>Hf</sub> (0)	ε <sub>Hf</sub> (t)	T <sub>DM1</sub>	T <sub>DM2</sub>
PM07-2											
1	166	0.040515	0.002037	0.000670	0.000023	0.282746	0.000019	-0.94	2.64	711	1041
2	166	0.061467	0.000448	0.000992	0.000008	0.282726	0.000028	-1.62	1.91	745	1088
3	165	0.150114	0.004686	0.001820	0.000053	0.282799	0.000026	0.94	4.37	657	931
4	911	0.035071	0.000337	0.000565	0.000003	0.281967	0.000026	-28.46	-8.67	1786	2319
5	167	0.075929	0.001397	0.001214	0.000021	0.282726	0.000023	-1.63	1.90	749	1089
6	167	0.051081	0.000408	0.000852	0.000002	0.282700	0.000022	-2.54	1.03	779	1144
7	165	0.045439	0.002054	0.000826	0.000044	0.282700	0.000018	-2.53	1.01	778	1144
8	166	0.025907	0.000612	0.000484	0.000007	0.282668	0.000022	-3.67	-0.08	815	1214
9	166	0.076393	0.000596	0.001292	0.000016	0.282371	0.000023	-14.18	-10.69	1254	1884
10	606	0.031990	0.000547	0.000534	0.000012	0.282639	0.000022	-4.69	8.47	857	1010
11	915	0.067331	0.000968	0.001279	0.000015	0.282063	0.000021	-25.08	-5.63	1686	2133
12	172	0.031692	0.000455	0.000648	0.000018	0.282682	0.000017	-3.20	0.51	801	1181
13	165	0.071802	0.000717	0.001268	0.000009	0.282664	0.000021	-3.81	-0.32	838	1229
14	166	0.042461	0.000503	0.000818	0.000008	0.282767	0.000020	-0.18	3.38	684	994
15	166	0.050142	0.001218	0.001071	0.000043	0.282684	0.000019	-3.10	0.42	805	1182
16	165	0.085432	0.004657	0.001617	0.000089	0.282721	0.000025	-1.79	1.66	764	1103
17	532	0.014854	0.000138	0.000264	0.000004	0.282131	0.000019	-22.68	-11.07	1549	2183
18	166	0.037516	0.000811	0.000682	0.000015	0.282678	0.000022	-3.32	0.26	806	1193
19	221	0.080903	0.001981	0.001365	0.000040	0.282308	0.000023	-16.40	-11.75	1345	1992
20	165	0.180642	0.002065	0.003109	0.000095	0.282800	0.000028	0.99	4.28	679	937

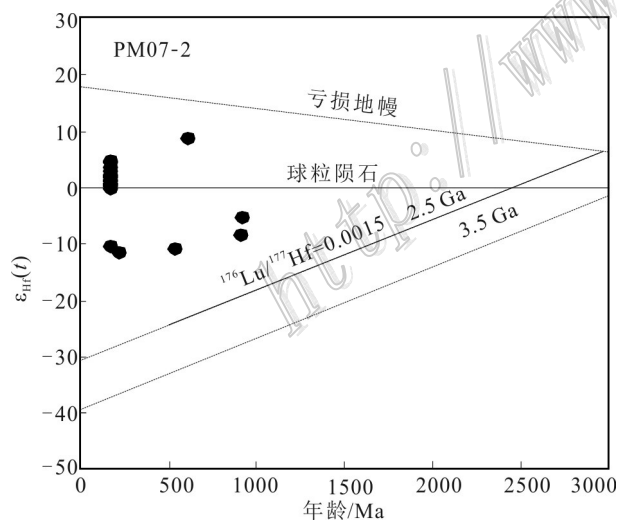


图 6 铁厂河花岗岩中锆石年龄-ε<sub>Hf</sub>(t)图解

Fig.6 ε<sub>Hf</sub>(t) versus age diagrams for zircons from the Teichanghe granite

样品中 Re 的含量变化较大, w(Re)为(3.904±0.032~20.86±0.15)×10<sup>-6</sup>。7 件辉钼矿 Re-Os 等时线年龄为

表 3 乌拉溪大牛场钨钼矿床中辉钼矿电子探针成分

Table 3 Electron probe analysis of molybdenite from the Daniuchang W-Mo deposit in Wulaxi region

编号	w(B)/%				总和
	Mo	Re	S	Os	
THQ-P2-1	55.576	0.073	41.487	0.134	97.271
THQ-P2-2	56.112	0.089	41.759	0.014	97.973
THQ-P2-3	55.407	0.111	42.480	0.032	98.030

(166.0±2.3) Ma (MSWD=1.5), 加权平均年龄为(166.8±1.7)Ma (MSWD=0.90)。

## 5 讨论

### 5.1 成岩成矿时代

矿床的精确定年是建立矿床模型和反演成矿地球动力学背景的基础,对于理解矿床的形成过程,确定矿床的成因,探讨成矿事件与其他地质事件的耦合关系,以及成矿-找矿模型的确立具有至关重要的

表4 乌拉溪大牛场钨钼矿床中辉钨矿 Re-Os 同位素数据

Table 4 Re-Os isotopic data of molybdenite from the Daniuchang W-Mo deposit in Wulaxi region

编号	m/g	$w(\text{Re})/10^{-6}$		$w(\text{普Os})/10^{-9}$		$w(^{187}\text{Re})/10^{-6}$		$w(^{187}\text{Os})/10^{-9}$		模式年龄/Ma	
		测定值	不确定度	测定值	不确定度	测定值	不确定度	测定值	不确定度	测定值	不确定度
WIX-M1	0.05	15.52	0.13	2.957	0.059	9.757	0.083	26.69	0.21	164.0	2.3
WIX-M2	0.03	16.75	0.13	2.526	0.029	10.53	0.08	28.83	0.23	164.2	2.3
WIX-M5	0.03	19.85	0.19	3.585	0.042	12.48	0.12	34.46	0.27	165.5	2.5
WIX-M6	0.03	20.86	0.15	2.482	0.022	13.11	0.10	36.95	0.29	168.9	2.3
WIX-M7	0.03	18.59	0.15	2.101	0.024	11.68	0.10	32.92	0.27	168.9	2.4
WIX-M8	0.10	4.445	0.034	0.1039	0.0037	2.794	0.021	7.867	0.062	168.8	2.3
WIX-M9	0.10	3.904	0.032	0.0757	0.0035	2.454	0.020	6.847	0.057	167.3	2.4

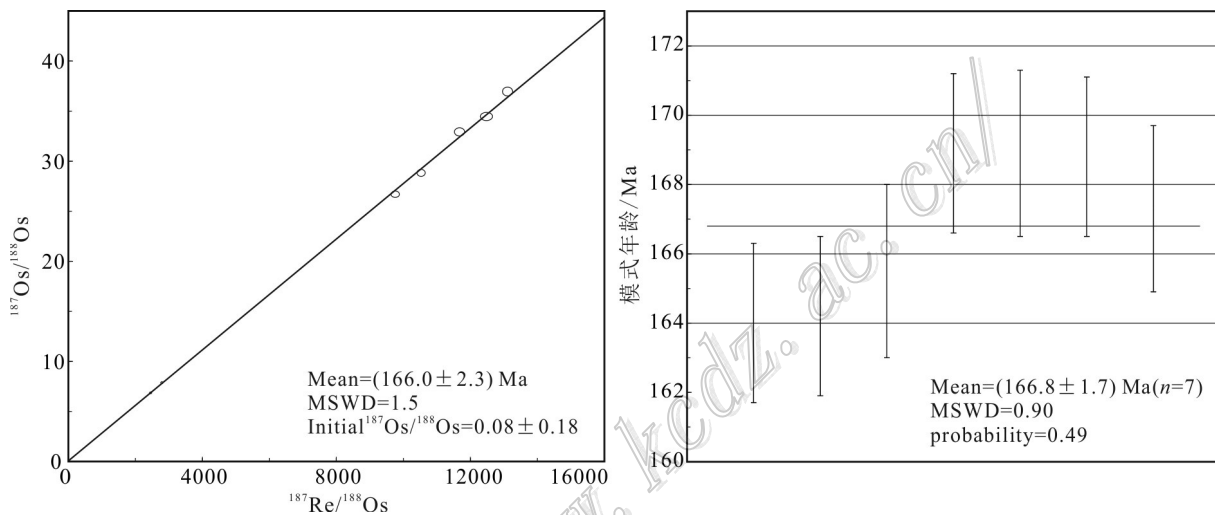


图7 乌拉溪大牛场辉钨矿 Re-Os 等时线及加权平均年龄图

Fig7 The diagrams of molybdenite Re-Os isochron age and weighted average age of the Daniuchang W-Mo deposit in Wulaxi region

意义(刘玉平等,2007;谭洪旗等,2011)。

松潘-甘孜地块北缘雪宝顶白钨矿 Sm-Nd 等时线年龄为(182.0±9.2)Ma(刘琰等,2007),康定县赫德钨锡矿床中辉钨矿 Re-Os 同位素年龄为(211.9±6.5)~(213.3±2.9)Ma(杨涛等,2017)。本文获得乌拉溪大牛场地区矽卡岩型辉钨矿 Re-Os 加权平均值为(166.8±1.7)Ma,与铁厂河花岗岩 LA-ICP-MS 锆石 U-Pb 年龄((166.0±0.9) Ma)在误差范围内基本一致(Tan, 2014;李同柱等,2016b)。上述年龄均证实了大牛场辉钨矿形成于燕山早期与花岗岩有关的矽卡岩矿床,与雪宝顶 W-Sn-Be 矿床和赫德钨锡矿床的成矿年龄略有差异,暗示九龙地区在~166 Ma 发生了与 W-Mo 矿化事件有关的岩浆活动。

锆石 Hf 同位素显示其模式年龄变化于 1884~931 Ma 之间,为 1229~931 Ma(平均 1099 Ma)和 1884 Ma。研究显示,扬子地块西缘会理群可能形成

于 1.1~1.0 Ga(Cui et al., 2021),扬子地块北西缘的鱼洞子杂岩中斜长角闪岩的变质年龄为(1848±5) Ma(Hui et al., 2017),且崆岭杂岩体发现有 1.85 Ga 的 A<sub>2</sub> 花岗岩及 1.78~1.85 Ga 的基性岩脉(邓奇等,2017)。因此,本文中获得的继承锆石 Hf 二阶段模式年龄显示了该花岗岩的物质源区可能为扬子地块基底古元古代与中元古代地壳重熔形成的。

## 5.2 花岗岩成因类型与钨钼矿床的关系

大牛场钨钼矿床与铁厂河花岗岩体在空间上密切相关,主要岩性为正长花岗岩和二长花岗岩。岩石地球化学分析表明,铁厂河岩体具有高 SiO<sub>2</sub>、Na<sub>2</sub>O 和 K<sub>2</sub>O 含量,高 FeO<sub>t</sub>/MgO、Ga/Al 比值,以及低 TiO<sub>2</sub>、CaO 和 MgO 含量特征,为铝质 A 型花岗岩(周家云等,2014a)。A 型花岗岩主要形成于伸展的构造背景,为碱性、贫水、非造山和铝质花岗岩(Loiselle et al., 1979),以高硅、富碱、低钙为特征,具有高温的特

点(吴福元等,2017)。A型花岗岩主要与锡、锆、钨、铌、钽及稀土矿产有关(Dall'Agnolet al.,2012)。前人研究认为,与钨矿化有关的岩浆岩多为陆壳重熔S型花岗岩,松潘-甘孜地块北缘雪宝顶W-Sn-Be矿床证实与A型花岗岩密切相关(刘琰等,2007),而铁厂河花岗岩也被证实为A型花岗岩(周家云等,2014a)。因此,A型花岗岩也可以是钨钼矿床的成矿母岩。

### 5.3 构造背景及地质意义

#### 5.3.1 构造背景

已报道的松潘-甘孜地区的花岗岩成岩年龄以220~205 Ma为主,大多为I型花岗岩和S型花岗岩(胡健民等,2005;Zhang et al.,2006;2007;Weislogel,2008;Xiao et al.,2007;Yuan et al.,2010;蔡宏明等,2010;Roger et al.,2004;2010;Sigoyer et al.,2014;Chen et al.,2017;刘大明,2018;Fei et al.,2020;Yan et al.,2020;Zhan et al.,2020),而年保玉花岗岩则为A型花岗岩(Zhang et al.,2007);少量花岗岩为165~150 Ma(Wallis et al.,2003;周家云等,2013;2014a;李同柱等,2016a;Dai et al.,2017;朱玉娣等,2018;谭洪旗,2019),且为A型花岗岩(周家云等,2013;2014a)。九龙乌拉溪大牛场地区的成岩成矿事件,与松潘-甘孜地体220~205 Ma时地壳碰撞收缩增厚晚约40 Ma左右,代表了印支期挤压向燕山期伸展体制转换的年龄限制。

区域背景显示,甘孜-理塘洋向西俯冲闭合峰期年龄约为216 Ma(吴涛,2015),与松潘-甘孜地区岩浆活动的216 Ma年龄峰一致(Wang et al.,2011),代表了松潘-甘孜地区的碰撞造山过程的挤压环境。江浪地区出露的基性岩脉变质年龄限制为214~206 Ma,代表造山事件的结束,也是松潘-甘孜地区岩石圈地壳加厚的结束(谭洪旗,2019)。本文获得铁厂河花岗岩年龄约为166 Ma,代表松潘-甘孜地块南缘岩石圈伸展的高峰期,形成于松潘-甘孜造山带收缩逆冲-滑脱(碰撞造山)之后,即岩石圈热隆伸展的开始(周家云等,2014a;许志琴等,1992)。因此,铁厂河花岗岩体是松潘-甘孜地块从印支期挤压向燕山早期伸展构造环境转换的产物,也是区域上特提斯构造域向太平洋构造域转换的关键时间节点。

#### 5.3.2 地质意义

以铁厂河花岗岩为代表的A型花岗岩,代表了九龙地区166~150 Ma期间处于伸展的构造背景。这种背景下,花岗岩浆的多次幕式活动,为江浪穹隆抬升和剥露提供了基础和动力。乌拉溪花岗岩中W、Mo等成矿元素含量较高,是本区主要的成矿岩体,为钨钼矿床的形成提供了热源和物源。燕山期,铁厂河花岗岩体侵入地层中产生热接触变质和交代作用,在接触界面上形成矽卡岩。前已交代,三叠系扎尕山组地层提供钙,花岗岩体提供钨、钼等成矿元素,即在矽卡岩带上或附近形成白钨矿和辉钼矿等

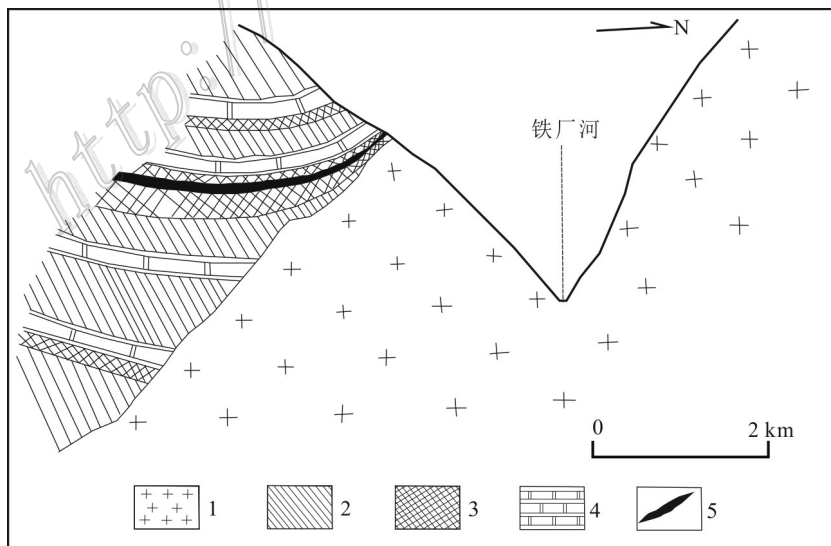


图8 矽卡岩带及矿体剖面示意图(据张伟民,1974修改)

1—铁厂河花岗岩;2—矽卡岩化角岩;3—矽卡岩;4—大理岩;5—矿体

Fig. 8 Schematic geologic section showing the skarn and orebody(modified after Zhang, 1974)

1—Tiechanghe granite; 2—Skarn-hornfels; 3—Skarn; 4—Marble; 5—Orebody

矿石矿物(图8)。

前人研究认为,矽卡岩型钨钼矿成矿深度为2~4 km(任云生等,2004;丁存根等,2009;田坎等,2018)。而铁厂河花岗岩中锆石和磷灰石裂变径迹显示,铁厂河花岗岩体抬升剥露深度大约为2170 m(谭洪旗,2019),已达到钨钼矿床成矿深度,暗示区内钨钼矿体有可能遭受隆升剥蚀作用。野外地质调查显示,矽卡岩型白钨矿矿体下方的坡积物中发现大量的白钨矿矿物,正是上述矿体遭受剥蚀的证据之一(谭洪旗等,2013)。因此,应加强九龙江浪穹隆及其外围铜锌-钨钼矿的找矿勘探工作,同时也应考虑九龙地区隆升剥蚀和深切割带来的影响,钨钼矿体可能因抬升剥露而消失殆尽。这一发现为江浪地区及其周缘找矿工作提供了新的思路。

## 6 结 论

(1) 确定了大牛场矽卡岩型钨钼多金属矿床形成年龄为(166.8±1.7)Ma。这一年龄与铁厂河花岗岩 LA-ICP-MS 锆石 U-Pb 年龄((166.0±0.9)Ma)在误差范围内基本一致,反映研究区~166 Ma 存在一期与花岗岩相关的 W-Mo 成矿事件。

(2) 花岗岩的 Hf 同位素表明与钨钼成矿有关花岗岩的物源为古元古代和中元古代地壳重熔形成的。

(3) 铁厂河花岗岩和钨钼成岩成矿时代与松潘-甘孜地块南缘岩石圈伸展的高峰期一致,是松潘-甘孜地块从印支期挤压向燕山早期伸展构造环境转换期的产物,也是特提斯构造域向太平洋构造域转换在九龙地区的成岩成矿响应。

**致 谢** 龚大兴博士和王越工程师参加了部分野外地质调查工作,锆石 U-Pb 定年和 Hf 同位素得到了中国地质科学院矿产资源研究所侯可军博士的帮助,辉钼矿 Re-Os 定年由国家测试中心李超副研究员完成,电子探针测试由中国地质科学院矿产综合利用研究所王越工程师完成,审稿专家和编辑提出了诸多建设性的意见,在此衷心表示感谢。

## References

Cai H M, Zhang H F, Xu W C, Shi Z L and Yuan H L. 2010. Petrogenesis of Indosinian volcanic rocks in Songpan-Garze fold belt of the

northeastern Tibetan Plateau: New evidence for lithospheric delamination[J]. *Science China Earth Science*, 53: 1316-1328.

Cai Q R, Yan Y F, Yang G S, Jia F J, Cui D H and Li C. 2018. Evolution of scheelite skarn mineralization at Nanyangtian deposit, southeast Yunnan Province[J]. *Mineral Deposits*, 37(1): 116-136(in Chinese with English abstract).

Chang Z S, Shu Q H and Meinert L D. 2019. Skarn deposits of China[A]. In: Chang Z S, Goldfarb R J, ed. *Mineral deposits of China*[M]. Society of Economic Geologists, SEG Special Publications. No. 22: 189-234.

Chen Q, Sun M, Zhao G C, Yang F L, Long X P, Li J H, Wang J and Yu Y. 2017. Origin of the mafic microgranular enclaves (MMEs) and their host granitoids from the Tagong pluton in Songpan-Ganze terrane: An igneous response to the closure of the Paleo-Tethys Ocean[J]. *Lithos*, 290-291: 1-17.

Cui X Z, Lin S F, Wang J, Ren G M, Su B R, Chen F L, Deng Q and Pang W H. 2021. Latest Mesoproterozoic provenance shift in the southwestern Yangtze Block, South China: Insights into tectonic evolution in the context of the supercontinent cycle[J]. *Gondwana Research*, 99: 131-148.

Dai Y P, Zhu Y D, Li T Z, Zhang H H, Tang G L and Shen Z W. 2017. A crustal source for ca. 165 Ma post-collisional granites related to mineralization in the Jianglang dome of the Songpan-Ganzi Orogen, eastern Tibetan Plateau[J]. *Geochemistry*, 77(4): 573-586.

Dall'Agnol R, Frost C D and Tapani Rämö O. 2012. IGCP Project 510 "A-type granites and related rocks through time": Project vita, results, and contribution to granite research[J]. *Lithos*, 151: 1-16.

Deng Q, Wang Z J, Wang J, Cui X Z, Ma L and Xiong X H. 2017. Discovery of the Baiyu ~1.79 Ga A-type granite in the Beiba area of the northwestern margin of Yangtze Block: Constraints on tectonic evolution of South China[J]. *Acta Geologica Sinica*, 91(7): 1454-1466(in Chinese with English abstract).

Ding C G, Zhang S G, Ma C and Xu Z F. 2009. Genetic mineralogical properties of sphalerite and discussions on its geobarometer application in skarn ore deposits in middle Ningzhen region[J]. *Journal of Geology*, 33(2): 124-129(in Chinese with English abstract).

Du A D, Qu W J, Wang D H and Li C. 2012. Rhenium osmium method and application in metallogenic chronology of Re-Os isotope[M]. Beijing: Geological Publishing House. 1-182(in Chinese).

Fei G C, Menuge J F, Li Y Q, Yang J Y, Deng Y, Chen C S, Yang Y F, Yang Z, Qin L Y, Zheng L and Tang W C. 2020. Petrogenesis of the Lijiagou spodumene pegmatites in Songpan-Garze Fold Belt, West Sichuan, China: Evidence from geochemistry, zircon, cassiterite and coltan U-Pb geochronology and Hf isotopic compositions[J]. *Lithos*, 364-365: 1-18.

Hou K J, Li Y H and Tian Y R. 2009. In situ U-Pb zircon dating using laser ablation-multiion counting-ICP-MS [J]. *Mineral Deposits*, 28(4): 481-492(in Chinese with English abstract).

Hou L W. 1996. Type and origin of the core complexes and the domal deformational-metamorphic bodies in the western margin of Yangtze Craton[J]. *Acta Geologica Sichuan*, 16(1): 6-11(in Chinese

- with English abstract).
- Hou Li W and Fu X F. 2002. The domal metamorphic bodies in the eastern margin of Songpan Ganzi orogenic belt[M]. Chengdu: Sichuan University Press. 137-142(in Chinese).
- Hu J L, Tan H Q, Zhou X, Ni Z Y and Zhou Y. 2020. A study of mineralogy and mineral chemistry of ore-bearing pegmatites in the Daqianggou lithium-beryllium deposit, western Sichuan[J]. Geological Bulletin of China, 39(12): 2013-2028(in Chinese with English abstract).
- Hu J M, Meng Q R, Shi Y R and Qu H J. 2005. SHRIMP U-Pb dating of zircons from granitoid bodies in the Songpan-Ganzi terrane and its implications[J]. Acta Petrological Sinica, 21(3): 867-880(in Chinese with English abstract).
- Hui B, Dong Y P, Cheng C, Long X P, Liu X M, Yang Z, Sun S S, Zhang F F and Varga J. 2017. Zircon U-Pb chronology, Hf isotope analysis and whole-rock geochemistry for the Neoproterozoic Yudongzi complex, northwestern margin of the Yangtze Craton, China[J]. Precambrian Research, 301: 65-85.
- Jiang S Y, Zhao K D, Jiang H, Su H M, Xiong S F, Xiong Y Q, Xu Y M, Zhang W and Zhu L Y. 2020. Spatiotemporal distribution, geological characteristics and metallogenic mechanism of tungsten and tin deposits in China: An overview[J]. China Science Bulletin, 65: 3730-3745.
- Li T Z, Dai Y P, Ma G T and Zhou Q. 2016a. SHRIMP zircon U-Pb dating of the Wulaxi granite in the western margin of the Yangtze Block and its geological significance[J]. Bulletin of Mineralogy, Petrology and Geochemistry, 35(4): 743-749(in Chinese with English abstract).
- Li T Z, Zhou Q, Zhang H H, Dai Y P, Ma G T, Ma D and Shen Z W. 2016b. Ore geology and molybdenite Re-Os dating of the Wulaxi tungsten deposit in western Sichuan[J]. Geological Journal of China Universities, 22(3): 423-430(in Chinese with English abstract).
- Liu D M. 2018. Geochemical composition, chronology and tectonic significances of Sanyanlong-Galazi granites in the southern Songpan-Garze orogenic Belt (dissertation for Master degree)[D]. Supervisor: Yin F G. Chengdu: Chengdu University of Technology. 60p(in Chinese with English abstract).
- Liu X J and Xu Z Q. 2021. Tectonic significance of Middle Jurassic granite in the Jianglang dome, southern Songpan-Ganzi Orogen Belt[J]. Acta Geological Sinica, 95(6): 1754-1773(in Chinese with English abstract).
- Liu Y P, Li Z X, Li H M, Guo L G, Xu W, Ye L, Li C Y and Pi D H. 2007. U-Pb geochronology of cassiterite and zircon from Dulong Sn-Zn deposit: Evidence for Cretaceous large-scale granitic magmatism and mineralization events in southeastern Yunnan Province, China[J]. Acta Petrologica Sinica, 23(5): 967-976(in Chinese with English abstract).
- Liu Y S, Hu Z C, Gao S, Gunther D, Xu J, Gao C G and Chen H H. 2008. In situ analysis of major and trace elements of anhydrous minerals by LA-ICP-MS without applying an internal standard[J]. Chemical Geology, 257(1-2): 34-43.
- Liu Y, Deng J, Li C F, Shi G H and Zheng A L. 2007. REE composition in scheelite and scheelite Sm-Nd dating for the Xuebaoding W-Sn-Be deposit in Sichuan[J]. Chinese Science Bulletin, 52(18): 2543-2550(in Chinese with English abstract).
- Liu Y, Deng J, Shi G H, Sun X and Yang L Q. 2012. Genesis of the Xuebaoding W-Sn-Be crystal deposits in southwest China: Evidence from fluid inclusions, stable isotopes and ore elements[J]. Resources Geology, 62(2): 159-173.
- Loiselle M C and Wones D R. 1979. Characteristics of anorogenic granite[J]. Geological Society of America. Abstracts with Programs, 11: 468.
- Ludwig K R. 2003. User's manual for isotopic 3.0: A geochronological toolkit for Microsoft excel[M]. Berkeley: Berkeley Geochronology Center. Special Publication No.4. 25-32.
- Luo L P, Hu J L, Tan H Q and Zhou T. 2021. Mineralogical characteristics of the pegmatite type beryl in Shangjigong, western Sichuan Province[J]. Multipurpose Utilization of Mineral Resources, 5: 113-119(in Chinese with English abstract).
- Ma G T, Yao P, Ma D F, Gao D F, Wang M J, Li J Z, Zhang H H, Chen M H and Liang J. 2012. LA-ICP-MS zircon U-Pb dating and geological implications for the Xinhuoshan granites in Jiulong, western Sichuan[J]. Sedimentary Geology and Tethyan Geology, 32(4): 70-75(in Chinese with English abstract).
- Mao J W, Li H Y, Guy B and Raimbault L. 1996. Geology and metallogeny of the Shizhuyuan skarn-greisen W-Sn-Mo-Bi deposit, Hunan Province[J]. Mineral Deposits, 15(1): 1-15(in Chinese with English abstract).
- Mao J W, Ouyang H G, Song S W, Santosh M, Yuan S D, Zhou Z H, Zheng W, Liu H, Liu P, Cheng Y B and Chen M H. 2019. Geology and metallogeny of tungsten and tin deposits in China[J]. In: Chang Z S, Goldfarb R J, ed. Mineral deposits of China[M]. Society of Economic Geologists, SEG Special Publications. No. 22: 411-482p.
- Ren Y S, Liu L D, Wan X Z and Liu L G. 2004. Discussion on the metallogenic depth of skarn type gold deposits in Tongling area, Anhui Province[J]. Geotectonica et Metallogenia, 28(4): 397-403 (in Chinese with English abstract).
- Roger F, Jolivet M and Malavieille J. 2010. Tectonic evolution of the Songpan-Garze (North Tibet) and adjacent areas from Proterozoic to present: A synthesis[J]. Journal of Asian Earth Sciences, 39: 254-269.
- Roger F, Malavieille J, Leloup P H, Calassou S and Xu Z. 2004. Timing of granite emplacement and cooling in the Songpan-Garze fold belt (eastern Tibetan plateau) with tectonic implication[J]. Journal of Asian Earth Science, 22: 465-481.
- Rong J S and Wang F G. 2016. Metasomatic textures in granites: Evidence from petrographic observation[M]. Beijing: Science Press and Springer Science + Business Media Singapore. 73-83.
- Sheng J F, Chen Z H, Liu L J, Ying L J, Huang F, Wang D H, Wang J H and Zeng L. 2015. Outline of metallogeny of tungsten deposits in China[J]. Acta Geologica Sinica, 89(6): 1038-1050(in Chinese

- with English abstract).
- Shirey S B and Walker R J. 1995. Carius tube digestion for low-blank rhenium-osmium analysis[J]. *Analytical Chemistry*, 67: 2136-2141.
- Shuang Y, Gong Y C, Li H, Tian X F, Mao L L and Chen W. 2016. Fluid-inclusion geochemistry of the large-sized Xintianling tungsten deposit, Hunan Province, China[J]. *Geochimica*, 45(6): 569-581 (in Chinese with English abstract).
- Sigoyer J D, Vanderhaeghe O, Duchêne S and Billerot A. 2014. Generation and emplacement of Triassic granitoids within the Songpan Ganze accretionary-orogenic wedge in a context of slab retreat accommodated by tear faulting, eastern Tibetan Plateau, China[J]. *Journal of Asian Earth Sciences*, 88: 192-216.
- Tan H Q, Liu Y P, Xu W, Guo L G, Ye L and Li C Y. 2011.  $^{40}\text{Ar}$ - $^{39}\text{Ar}$  dating of phlogopite from W-Sn deposits in the Nanyangian, southeastern Yunnan, and its implication[J]. *Acta Mineralogica Sinica*, 31(S): 639-640(in Chinese).
- Tan H Q, Zhou J Y, Zhu Z M, Zhang Y, Gong D X, Zhou X and Luo L P. 2012. Geological setting and prospecting direction of Wulaxi scheelite deposit in Jiulong, Sichuan Province[J]. *Mineral Deposits*, 31(s1): 1213(in Chinese).
- Tan H Q, Zhou J Y, Zhu Z M, Luo L P, Gong D X and Zhou X. 2013. Extension process and metallogenic effect of Jianglang dome, western Sichuan Province[J]. *Acta Mineralogica Sinica*, 32(S2): 961(in Chinese).
- Tan H Q. 2014. Re-Os dating of molybdenites and its geological significance in the Jianglang dome, SW China[J]. *Acta Geologica Sinica (English Edition)*, 88(Supp.2): 928.
- Tan H Q, Luo L P, Zhou J Y, Zhu Z M, Gong D X and Liu Y D. 2016. Discovery of Qingna gold deposit in Jinping area and its geological significance, western Sichuan[J]. *Science Technology and Engineering*, 21(16): 12-19(in Chinese with English abstract).
- Tan H Q. 2019. The composition, deformation-metamorphic characteristics and metallogenic response of the dome geological bodies on the south margin of Songpan-Garze Block (dissertation for Doctor degree)[D]. Supervisor: Ni Z Y. Chengdu: Chengdu University of Technology. 194-195(in Chinese with English summary).
- Tian K, Zheng Y Y, Gao S B, Wu D H and Jiang X J. 2018. Fluid source and evolution of the Bangbule skarn Pb-Zn-Cu-Fe deposit in Tibet: Constraints from fluid inclusions and stable isotopes[J]. *Geotectonica et Metallogenia*, 42(6): 1027-1045(in Chinese with English abstract).
- Wallis S, Tsujimori T, Aoya M, Kawakami T, Terada K, Suzuki K and Hyodo H. 2003. Cenozoic and Mesozoic metamorphism in the Longmenshan orogeny: Implication for geodynamic model of eastern Tibet[J]. *Geology*, 31(9): 745-758.
- Wan C H, Yuan J, Li F X and Yan S W. 2011. Late Triassic granitoids in the southern part of the Songpan-Garze Fold Belt: Petrology, geochemical composition and petrogenesis[J]. *Acta Petrologica et Mineralogica*, 30(2): 185-198(in Chinese with English abstract).
- Wang P, Pan Z L and Weng L B. 1982. Systematic mineralogy[M]. Beijing: Geological Publishing House. 389-390(in Chinese).
- Wang Q, Li Z X, Chung S L, Wyman D A, Sun Y L, Zhao Z H, Zhu Y T and Qiu H N. 2011. Late Triassic high-Mg andesite/dacite suites from northern Hohxil, North Tibet geochronology, geochemical characteristics, petrogenetic processes and tectonic implications[J]. *Lithos*, 126(2): 54-67.
- Weislogel A L. 2008. Tectonostratigraphic and geochronologic constraints on evolution of the northeast Paleo Tethys from the Songpan-Ganzi complex, central China[J]. *Tectonophysics*, 451(1-4): 331-345.
- Wu F Y, Liu X C, Ji W Q, Wang J M and Yang L. 2017. Highly fractionated granites: Recognition and research[J]. *Science China Earth Sciences*, 60: 1201-1219.
- Wu T. 2015. Early Mesozoic magmatism and tectonic evolution (dissertation for doctor degree) [D]. Supervisor: Xiao L. Wuhan: China University of Geosciences (Wuhan). 89p(in Chinese with English summary).
- Xiao L, Zhang H F, Clemens J D, Wang Q W, Kan Z Z, Wang K M, Ni P Z and Liu X M. 2007. Late Triassic granitoids of the eastern margin of the Tibetan Plateau: Geochronology, petrogenesis and implications for tectonic evolution[J]. *Lithos*, 96(3-4): 436-452.
- Xiao Q L, Wang X Q, Liu Z Z, Li T F and Feng L. Tungsten metallogenic geological features and mineral resources potential analyses in China[J]. *Earth Science Frontiers*, 25(3): 50-58(in Chinese with English abstract).
- Xu Z Q, Hou L W, Wang Z X, Fu X F and Huang M H. 1992. Orogenic process of Songpan-Ganzi orogenic belt in China[M]. Beijing: Geological Publishing House. 170-182(in Chinese).
- Yan D P, Song H L and Fu Z R. 1997. Tectono-stratigraphic division foreexposed crust section of Jianglangmetamorphic core complex in western margin of Yangtze Craton[J]. *Geoscience*, 11(3): 290-297(in Chinese with English abstract).
- Yan Q G, Li J K, Li X J, Liu Y C, Li P and Xiong X. 2020. Source of the Zhawulong granitic pegmatite-type lithium deposit in the Songpan-Ganze orogenic belt, western Sichuan, China: Constraints from Sr-Nd-Hf isotopes and petrochemistry[J]. *Lithos*, 378-379: 1-11.
- Yang T, Xin C L and An G B. 2017. Geological characteristics and genesis of Hede tungsten-tin deposition Kangding County, Sichuan Province[J]. *Contributions to Geology and Mineral Resource Research*, 32(14): 562-569(in Chinese with English abstract).
- Yuan C, Zhou M F, Sun M, Zhao Y J, Wilde S, Long X P and Yan D P. 2010. Triassic granitoids in the eastern Songpan Ganzi Fold Belt, SW China: Magmatic response to geodynamics of the deep lithosphere[J]. *Earth and Planetary Science Letters*, 290(3-4): 481-492.
- Yuan J, Xiao L, Wan C H and Gao R. 2011. Petrogenesis of Fangmaying-Sanyanlong granites in southern Songpan-Garze Fold Belt and its tectonic implication[J]. *Acta Geologica Sinica*, 85(2): 195-206(in Chinese with English abstract).
- Zhan Q Y, Zhu D C, Wang Q, Weinberg R F, Xie J C, Li S M, Zhang L L and Zhao Z D. 2020. Source and pressure effects in the genesis

- of the Late Triassic high Sr/Y granites from the Songpan-Ganzi Fold Belt, eastern Tibetan Plateau[J]. *Lithos*, 368-369: 1-15.
- Zhang H F, Parrish R, Zhang L, Xu W C, Yuan H L, Gao S and Crowley Q G. 2007. A-type granite and adakitic magmatism association in Songpan-Garze Fold Belt, eastern Tibetan Plateau: Implications for lithospheric delamination[J]. *Lithos*, 97(3-4): 323-335.
- Zhang H F, Zhang L, Harris N, Jin L L and Yuan H L. 2006. U-Pb zircon ages, geochemical and isotopic compositions of granitoids in Songpan-Garze Fold Belt, eastern Tibet Plateau: Constraints on petrogenesis, nature of basement and tectonic evolution[J]. *Contributions to Mineralogy and Petrology*, 152(1): 75-88.
- Zhang W M. 1974. Jinkuang 1/200,000 regional geological survey report (Mineral part) [R]. Xichang: The First Regional Geological Survey Brigade of Sichuan Geological Bureau. Unpublished report. 70p(in Chinese).
- Zhao Y M, Lin W W, Bi C S, Li D X and Jiang C J. 2012. Skarn deposits in China[M]. Beijing: Geological Publishing House. 2p(in Chinese).
- Zhou J Y, Tan H Q, Gong D X, Zhu Z M and Luo L P. 2013. Zircon LA-ICP-MS U-Pb dating and Hf isotopic composition of Xinhushan granite in the core of Jianglang dome, Western Sichuan, China[J]. *Journal of Mineralogy and Petrology*, 33(4): 42-52(in Chinese with English abstract).
- Zhou J Y, Tan H Q, Gong D X, Zhu Z M and Luo L P. 2014a. Wulaxi aluminous A-type granite in western Sichuan, China: Recording Early Yanshanian lithospheric thermo-upwelling extension of Songpan-Garze Orogenic Belt[J]. *Geological Review*, 60(2): 348-362(in Chinese with English abstract).
- Zhou J Y, Tan H Q and Luo L P. 2014b. Prospecting report of Wulaxiaojin area in Jiulong, Sichuan Province[R]. Chengdu: Institute of Multipurpose Utilization of Mineral Resources, Chinese Academy of Geological Sciences. Unpublished Report. 113-124(in Chinese).
- Zhou Q, Li W C, Zhang H H, Li T Z, Yuan H Y, Feng X L, Li C, Liao Z W and Wang S W. 2017. Post-magmatic hydrothermal origin of Late Jurassic Liwu copper polymetallic deposits, western China: Direct chalcopyrite Re-Os dating and Pb-B isotopic constraints[J]. *Ore Geology Reviews*, 89: 526-543.
- Zhu Y D, Dai Y P, Wang L L, Li T Z, Zhang H H and Shen Z W. 2018. Petrogenesis and geological significance of the Wenjiaping granite in Jianglang Dome, southern rim of Songpan-Garze Orogenic Belt[J]. *Geoscience*, 32(1): 16-27(in Chinese with English abstract).
- 附中文参考文献**
- 蔡宏明,张宏飞,徐旺春,时章亮,袁洪林. 2010. 松潘带印支期岩石圈折沉作用新证据:来自火山岩岩石成因的研究[J]. *中国科学(地球科学)*, 40(11): 1518-1532.
- 蔡倩茹,燕永锋,杨光树,贾福聚,崔东豪,李超. 2018. 滇东南南秧田矽卡岩型钨钼矿床成矿演化[J]. *矿床地质*, 37(1): 116-136.
- 邓奇,汪正江,王剑,崔晓庄,马龙,熊小辉. 2017. 扬子地块西北缘碑坝地区白玉~1.79 Ga A型花岗岩的发现及其对构造演化的制约[J]. *地质学报*, 91(7): 1454-1466.
- 丁存根,张术根,马春,徐忠发. 2009. 宁镇中段矽卡岩型矿床的闪锌矿及其地质压力计应用讨论[J]. *地质学刊*, 33(2): 124-129.
- 杜安道,屈文俊,王登红,李超. 2012. 铼-钨法及其在矿床学中的应用[M]. 北京:地质出版社. 1-182.
- 侯可军,李延河,田有荣. 2009. LA-MC-ICP-MS 锆石微区原位 U-Pb 定年技术[J]. *矿床地质*, 28(4): 481-492.
- 侯立玮. 1996. 扬子克拉通西缘穹窿状变形变质体的类型与成因[J]. *四川地质学报*, 16(1): 6-11.
- 侯立玮,付小方. 2002. 松潘—甘孜造山带东缘穹窿状变质地质体[M]. 成都:四川大学出版社. 137-142.
- 胡健民,孟庆任,石玉若,渠洪杰. 2005. 松潘-甘孜地体内花岗岩锆石 SHRIMP 定年及其构造意义[J]. *岩石学报*, 21(3): 867-880.
- 胡军亮,谭洪旗,周雄,倪志耀,周玉. 2020. 川西九龙打枪沟铋矿床赋矿伟晶岩矿物学和矿物化学特征[J]. *地质通报*, 39(12): 2013-2028.
- 蒋少涌,赵葵东,姜海,苏慧敏,熊索菲,熊伊曲,徐耀明,章伟,朱律运. 2020. 中国钨锡矿床时空分布规律、地质特征与成矿机制研究进展[J]. *科学通报*, 65(33): 3730-3745.
- 李同柱,代堰镔,马国桃,周清. 2016a. 扬子陆块西缘乌拉溪花岗岩体 SHRIMP 锆石 U-Pb 定年及地质意义[J]. *矿物岩石地球化学通报*, 35(4): 743-749.
- 李同柱,周清,张惠华,代堰镔,马国桃,马东,沈占武. 2016b. 川西乌拉溪钨矿床地质特征及辉钨矿 Re-Os 定年[J]. *高校地质学报*, 22(3): 423-430.
- 刘大明. 2018. 松潘-甘孜南部三岩龙-嘎拉子花岗岩体地球化学、年代学及构造意义(硕士论文)[D]. 导师:尹福光. 成都:成都理工大学. 60页.
- 刘晓佳,许志琴. 2021. 松潘-甘孜造山带南部江浪穹隆中侏罗世花岗岩及构造意义[J]. *地质学报*, 95(6): 1754-1773.
- 刘琰,邓军,李潮峰,施光海,郑爱力. 2007. 四川雪宝顶白钨矿稀土地球化学与 Sm-Nd 同位素定年[J]. *科学通报*, 52(16): 1923-1929.
- 刘玉平,李正祥,李惠民,郭利果,徐伟,叶霖,李朝阳,皮道会. 2007. 都龙锡矿床锡石和锆石 U-Pb 年代学:滇东南白垩纪大规模花岗岩成岩-成矿事件[J]. *岩石学报*, 23(5): 967-976.
- 罗丽萍,胡军亮,谭洪旗,周涛. 2021. 川西上基拱伟晶岩型铋矿绿柱石矿物化学特征[J]. *矿产综合利用*, 5: 113-119.
- 马国桃,姚鹏,马东方,高大发,汪名杰,李建忠,张慧华,陈敏华,梁鲸. 2012. 四川九龙新火山花岗岩体单颗粒锆石 LA-ICP-MS U-Pb 定年及其地质意义[J]. *沉积与特提斯地质*, 32(4): 70-75.
- 毛景文,李红艳, Guy B, Raimbault L. 1996. 湖南柿竹园矽卡岩-云英岩型 W-Sn-Mo-Bi 矿床地质和成矿作用[J]. *矿床地质*, 15(1): 1-15.
- 任云生,刘连登,万相宗,刘良根. 2004. 铜陵地区矽卡岩型独立金矿成矿深度探讨[J]. *大地构造与成矿学*, 28(4): 397-403.
- 盛继福,陈郑辉,刘丽君,应立娟,黄凡,王登红,王家欢,曾乐. 2015. 中国钨矿成矿规律概要[J]. *地质学报*, 89(6): 1038-1050.
- 双燕,龚业超,李航,田旭峰,毛玲玲,陈威. 2016. 湘南新田岭大型钨

- 矿流体包裹体地球化学特征[J]. 地球化学, 45(6): 569-581.
- 谭洪旗, 刘玉平, 叶霖, 李朝阳. 2011. 滇东南南秧田钨锡矿床金云母<sup>40</sup>Ar-<sup>39</sup>Ar定年及意义[J]. 矿物学报, 31(S1): 639-640.
- 谭洪旗, 周家云, 朱志敏, 张贻, 龚大兴, 周雄, 罗丽萍. 2012. 四川九龙乌拉溪白钨矿床地质背景及找矿方向[J]. 矿床地质, 31(s1): 1213.
- 谭洪旗, 周家云, 朱志敏, 罗丽萍, 龚大兴, 周雄. 2013. 川西江浪穹窿伸展过程及成矿效应[J]. 矿物学报, 32(S2): 961.
- 谭洪旗, 罗丽萍, 周家云, 朱志敏, 龚大兴, 刘应冬. 2016. 川西锦屏地区青纳金矿床的发现及地质意义[J]. 科学技术与工程, 21(16): 12-19.
- 谭洪旗. 2019. 松潘-甘孜地块南缘穹隆体物质组成、变形-变质特征及成矿响应(博士论文)[D]. 导师: 倪志耀. 成都: 成都理工大学. 194-195.
- 田坎, 郑有业, 高顺宝, 伍登浩, 姜晓佳. 2018. 西藏帮布勒砂卡岩型Pb-Zn-Cu-Fe矿床流体来源及演化: 来自流体包裹体及稳定同位素的制约[J]. 大地构造与成矿学, 42(6): 75-93.
- 万传辉, 袁静, 李芬香, 鄢圣武. 2011. 松潘-甘孜造山带南段晚三叠世兰尼巴和羊房沟花岗岩岩石学、地球化学特征及成因[J]. 岩石矿物学杂志, 30(2): 185-198.
- 王濮, 潘兆鲁, 翁玲宝. 1982. 系统矿物学[M]. 北京: 地质出版社. 389-390.
- 吴福元, 刘小驰, 纪伟强, 王佳敏, 杨雷. 2017. 高分异花岗岩的识别与研究[J]. 中国科学: 地球科学, 47: 745-765.
- 吴涛. 2015. 藏东义敦岛弧带早中生代岩浆活动与构造演化过程(博士论文)[D]. 导师: 肖龙. 武汉: 中国地质大学. 89页.
- 夏庆霖, 汪新庆, 刘壮壮, 李童斐, 冯磊. 2018. 中国钨矿成矿地质特征与资源潜力分析[J]. 地学前缘, 25(3): 50-58.
- 许志琴, 侯立玮, 王宗秀, 付小方, 黄明华. 1992. 中国松潘-甘孜造山带的造山过程[M]. 北京: 地质出版社. 170-182.
- 颜丹平, 宋鸿林, 傅昭仁. 1997. 扬子地台西缘江浪变质核杂岩的出露地壳剖面构造地层柱[J]. 现代地质, 11(3): 290-297.
- 杨涛, 辛存林, 安国堡. 2017. 四川省康定县赫德钨锡矿地质特征及矿床成因[J]. 地质找矿论丛, 32(14): 562-569.
- 袁静, 肖龙, 万传辉, 高睿. 2011. 松潘-甘孜南部放马坪-三岩花岗岩的成因及其构造意义[J]. 地质学报, 85(2): 195-206.
- 张伟民. 1974. 金矿幅1/20万区域地质调查报告(矿产部分)[R]. 西昌: 四川省地质局第一区域地质测量大队. 内部报告. 70页.
- 赵一鸣, 林文蔚, 毕承思, 李大新, 蒋崇俊. 2012. 中国砂卡岩矿床[M]. 北京: 地质出版社. 2页.
- 周家云, 谭洪旗, 龚大兴, 朱志敏, 罗丽萍. 2013. 川西江浪穹窿核部新火山花岗岩 LA-ICP-MS 锆石 U-Pb 定年和 Hf 同位素研究[J]. 矿物岩石, 33(4): 42-52.
- 周家云, 谭洪旗, 龚大兴, 朱志敏, 罗丽萍. 2014a. 乌拉溪铝质 A 型花岗岩: 松潘-甘孜造山带燕山早期热隆伸展的岩石记录[J]. 地质论评, 60(2): 348-362.
- 周家云, 谭洪旗, 罗丽萍. 2014b. 四川九龙乌拉-小金地区矿产远景调查报告[R]. 成都: 中国地质科学院矿产综合利用研究所. 内部报告. 113-124.
- 朱玉娣, 代堰铭, 王丽丽, 李同柱, 张惠华, 沈战武. 2018. 松潘-甘孜造山带南缘江浪穹窿文家坪花岗岩成因及地质意义[J]. 现代地质, 32(1): 16-27.